Eur. Phys. J. E **7**, 303–310 (2002)
DOI 10.1140/epje/i2001-10096-4

THE EUROPEAN PHYSICAL JOURNAL E
EDP Sciences

Why is nacre strong? II. Remaining mechanical weakness for cracks propagating along the sheets

K. Okumura[a]

Physique de la Matière Condensée, Collège de France, 11, place Marcelin-Berthelot, 75231 Paris cedex 05, France
Department of Physics, Graduate School of Humanities and Sciences, Ochanomizu University, 2-1-1, Otsuka, Bunkyo-ku, 112-8610, Japan

Received 16 November 2001

Abstract. In our previous paper (Eur. Phys. J. E **4**, 121 (2001)) we proposed a coarse-grained elastic energy for nacre, or stratified structure of hard and soft layers found in certain seashells . We then analyzed a crack running perpendicular to the layers and suggested one possible reason for the enhanced toughness of this substance. In the present paper, we consider a crack running parallel to the layers. We propose a new term added to the previous elastic energy, which is associated with the bending of layers. We show that there are two regimes for the parallel-fracture solution of this elastic energy; near the fracture tip the deformation field is governed by a parabolic differential equation while the field away from the tip follows the usual elliptic equation. Analytical results show that the fracture tip is lenticular, as suggested in a paper on a smectic liquid crystal (P.G. de Gennes, Europhys. Lett. **13**, 709 (1990)). On the contrary, away from the tip, the stress and deformation distribution recover the usual singular behaviors ($\sqrt{x}$ and $1/\sqrt{x}$, respectively, where x is the distance from the tip). This indicates there is no enhancement in toughness in the case of parallel fracture.

PACS. 87.68.+z Biomaterials and biological interfaces – 46.50.+a Fracture mechanics, fatigue and cracks – 81.07.-b Nanoscale materials and structures: fabrication and characterization

1 Introduction

A number of *living soft matters* derive their strength from some composite structures. Tooth and timber are among the examples. These composite structures have motivated studies mainly in the industry or technology-oriented field to produce strong materials, such as raw material for construction or air plane and automobile tires [1–3]. One of the purposes of this paper is to present some complementary understandings of such a problem from the viewpoint of a physicist, particularly of a special structure found in seashells such as abalone.

In the first of this series of papers [4], which deepened the scaling picture presented in [5], we studied nacre [6–9] which has an alternating laminated structure of hard and soft layers (Fig. 1). One of the significant features of this substance lies in the length scale of the layers. The thicknesses of the hard inorganic layer d_{h} and that of the soft organic layer d_{s} are of the order of nanometer and micron, respectively. This allows us a coarse-grained treatment in which an *average deformation field* may be well defined and can be used for the analysis of the field *even near the tip*. Simplifying the coarse-grained elastic

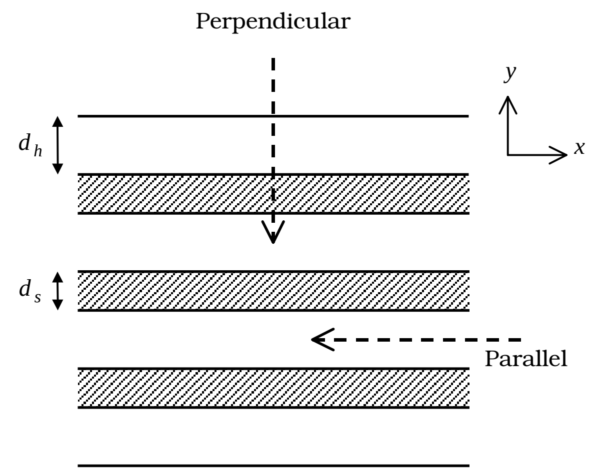

Fig. 1. Nacre structure: the (inorganic) hard-layer thickness d_{h} is of the order of the micrometer, while the (organic) soft-layer thickness d_{s} of the nanometer. The y-axis is perpendicular to layers and the sample is long in the z-direction. The cracks in the y-z plane and in the x-z plane are called the perpendicular and the parallel fractures, respectively.

energy further in terms of Fourier components of the deformation field, which is somewhat different from conventional approaches [3], we could show analytical solutions

[a] e-mail: okumura@phys.ocha.ac.jp

and thereby demonstrate one possible mechanism for the toughness of nacre for a perpendicular crack.

This paper does not concern the enhancement in toughness as suggested by the title. Rather, we proceed to study a case of parallel crack with the fixed grip condition from *the continuum view* (as for non-continuum treatment on laminated composites, see for example, [10]). As we will see later, this coarse-grained treatment again leads to a reasonably simplified picture of the problem. To describe the fields near the tip, we shall find that an extra term is required in our elastic energy. This term introduces a new length scale λ, as we see below, and this extra term becomes important near the tip ($x \ll \lambda$, where x is the distance from the tip). This term is suggested previously concerning some smectic liquid crystal [11] and a *lenticular* tip form is predicted from scaling arguments [12]. Here, we obtain an analytical solution to the stress and deformation distribution near the tip; the tip form in this case takes also the lenticular form. The appearance of a *parabolic* differential equation for the deformation field due to the extra term is another feature of this paper. We also obtain an analytical solution for $x \gg \lambda$, which allows us to estimate the fracture energy; there is no energy enhancement within our treatment.

The Young modulus of the hard and the soft layer are denoted E_h and E_s, respectively, where

$$E_\mathrm{s} = \varepsilon E_\mathrm{h}.$$

In the following, we consider the case of parallel fractures under the plane strain condition, *i.e.* $e_{zx} = e_{zy} = e_{zz} = 0$ (Fig. 1). Here, e_{ij} is the strain derived from the displacement field u_i, *i.e.*

$$e_{ij} = \frac{1}{2}\left(\frac{\partial u_i}{\partial x_j} + \frac{\partial u_j}{\partial x_i}\right),$$

where $(x_1, x_2, x_3) \equiv (x, y, z)$.

The ensuing analysis is based on the conditions appropriate for nacre:

$$\varepsilon \ll 1,$$

$$d_\mathrm{s} \ll d_\mathrm{h},$$

$$\epsilon = \varepsilon d/d_\mathrm{s} \ll 1,$$

where, $d = d_\mathrm{s} + d_\mathrm{h} \simeq d_\mathrm{h}$.

1.1 Elastic energy for the nacre in the thin layer limit

Assuming that the thickness of layers is thin in the sense that we can neglect the stress change over a few layers, we can introduce a *macroscopic strain field* to have the following elastic energy [4]:

$$f = \frac{E}{2(1-\nu^2)}e_{xx}^2 + \frac{E_0}{2}e_{yy}^2 + \frac{E_0}{1+\nu}e_{xy}^2 + \frac{\nu E_0}{1-\nu}e_{xx}e_{yy}, \quad (1)$$

where

$$E = E_\mathrm{h},$$

$$E_0 = \epsilon E_\mathrm{h}.$$

We have assumed that the Poisson ratio is the same for both layers for simplicity (even if $E_\mathrm{s} \gg E_\mathrm{h}$, or $\varepsilon \ll 1$, ν_s and ν_h are typically of the same order). We have checked (for the perpendicular crack) that the stress distribution resulting from this energy exhibits a small change over a few layers, which justifies the above assumption.

The strain-stress relation results from this energy by the relation $\sigma_{ij} = \partial f/\partial e_{ij}$:

$$\sigma_{xx} = \frac{E}{1-\nu^2}e_{xx} + \frac{\nu}{1-\nu}E_0 e_{yy}, \quad (2a)$$

$$\sigma_{yy} = E_0\left(e_{yy} + \frac{\nu}{1-\nu}e_{xx}\right), \quad (2b)$$

$$\sigma_{xy} = \frac{E_0}{1+\nu}e_{xy}. \quad (2c)$$

1.2 Parallel fracture: inclusion of the bending effect

Near the fracture tip, the stress gradient is large; we may need to include the stress changes within a single layer in some cases. In the case of parallel fracture, the bending, which originates from the nonuniform stress, is important as we see below. The correction due to the bending effect is given by (neglecting the bending energy of the soft layer)

$$f_\mathrm{B} = \frac{B_\mathrm{h}}{2d}\left(\frac{\partial^2 u_y}{\partial x^2}\right)^2 \equiv \frac{K}{2}\left(\frac{\partial^2 u_y}{\partial x^2}\right)^2,$$

where the bending modulus is given by [13]

$$B_\mathrm{h} = \frac{E_\mathrm{h} d_\mathrm{h}^3}{12(1-\nu^2)}.$$

The total energy is then given by

$$f_\mathrm{T} = f + \frac{K}{2}\left(\frac{\partial^2 u_y}{\partial x^2}\right)^2. \quad (3)$$

As we shall see later, in the case of parallel fracture, the first term in f in equation (1) becomes negligible; the remaining terms in f are all associated with the weak modulus E_s, while the bending term is associated with the strong modulus E_h. This suggests the possibility that *this higher-order derivative term makes a significant contribution to the energy in the parallel fracture.*

In accordance with the introduction of the bending term, we have another length scale λ as announced:

$$\lambda^2 = \frac{K}{E_0} \sim \frac{d^2}{\epsilon}.$$

2 Scaling prediction

As we see below, at large scale where $\lambda \ll x$, we have $u_x \ll u_y$, and the elastic energy is simplified to

$$f = \frac{E_0}{2}\left(\frac{\partial u_y}{\partial y}\right)^2 + \frac{E_0}{4(1+\nu)}\left(\frac{\partial u_y}{\partial x}\right)^2. \quad (4)$$

At small scale $\lambda \gg x$, we also have $u_x \ll u_y$ and the elastic energy is simplified to

$$f = \frac{E_0}{2}\left(\frac{\partial u_y}{\partial y}\right)^2 + \frac{K}{2}\left(\frac{\partial^2 u_y}{\partial x^2}\right)^2. \tag{5}$$

This energy in equation (5) has been discussed for smectic liquid crystals [11,12]. By considering *energy balance as in the Griffith theory* [14], it is predicted that the system exhibits a "lenticular fracture", where the opening angle θ_0 is *finite*, *i.e.*

$$\theta_0^2 \sim \frac{G_0}{E_0\lambda}, \tag{6}$$

where $G_0(= 2\gamma_0)$ is a thermodynamic separation energy for the soft medium (where γ_0 is the surface energy of the organic substance). Note here this angle is small ($\theta_0 \ll 1$) because $G_0/E_0 \sim a$, where a is a molecular length; thus we see the angle is small ($\theta_0^2 \sim a/\lambda$). (Here, the relation, $G_0/E_0 \sim a$, results from the following argument. The scaling expression for the elastic modulus for polymer melt is given by $E \sim cT/N_e$ where $c \sim 1/a^3$ and $N_e \sim 100$ [15], while the surface tension is typically given by $\gamma = T/a^2$ [16]. Thus, we have $E \sim \gamma/a$.)

In the inner (small-scale) region, the deformation of the free surface is given by

$$u_s \equiv u_y(x, y = 0) = \theta_0 x.$$

In the outer (large-scale) region where the bending term is neglected, we expect the usual singular behavior for the stress and deformation distribution because the deformation field satisfies the two-dimensional Laplace equation resulting from the energy in equation (4):

$$\sigma_s \equiv \sigma_{yy}(x, y = 0) = \frac{K_I}{\sqrt{-x}},$$
$$u_s = \frac{K_I}{E_0}\sqrt{x}.$$

Requiring the matching of the deformation field at $x = \lambda$, we have

$$K_I^2 = E_0^2\theta_0^2\lambda = G_0E_0.$$

This shows that the stress intensity factor is of the same order as that for a pure organic system; there is no enhancement of the separation energy.

K_I usually depends on the remote tensile stress and, at the moment of fracture (where $\sigma_\infty = \sigma_{\text{Failure}}$), the square of this coincides with the elastic constant multiplied by the fracture energy (*e.g.*, $K_I^2 = \mu G$). In the above, it seems that K_I does not depend on the remote stress from the beginning. This is because expression (6) is derived from an energy-balance consideration which requires the condition "at the moment of fracture."

3 Simplification of the energy at large and small scales

At equilibrium, by requiring $\delta F = F(u_x + \delta u_x) - F(u_x) = 0$ for any displacement δu_x, where

$$F = \int d\mathbf{r}\left(\frac{E}{2(1-\nu^2)}e_{xx}^2 + \frac{E_0}{2}e_{yy}^2 + \frac{E_0}{1+\nu}e_{xy}^2 + \frac{\nu E_0}{1-\nu}e_{xx}e_{yy} + \frac{K}{2}\left(\frac{\partial^2 u_y}{\partial x^2}\right)^2\right), \tag{7}$$

we have

$$\frac{\partial^2 u_x}{\partial x^2} + \epsilon\alpha\frac{\partial^2 u_x}{\partial y^2} + \epsilon\beta\frac{\partial^2 u_y}{\partial x\partial y} = 0,$$

where

$$\alpha = \frac{1}{2(1+\nu)}, \beta = \frac{1}{2}\left(\frac{1}{1+\nu} + \frac{2\nu}{1-\nu}\right).$$

For the displacement of u_y, we have

$$\frac{\partial^2 u_y}{\partial y^2} + \alpha\frac{\partial^2 u_y}{\partial x^2} + \beta\frac{\partial^2 u_x}{\partial x\partial y} - \lambda^2\frac{\partial^4 u_y}{\partial x^4} = 0.$$

Let us try to find a solution of the form

$$u_x = u\exp(ipx)\exp(iqy),$$
$$u_y = v\exp(ipx)\exp(iqy)$$

and put them into the above two equations. We have

$$\begin{pmatrix} p^2 + \epsilon\alpha q^2 & \epsilon\beta pq \\ \beta pq & q^2 + (\alpha + \lambda^2p^2)p^2 \end{pmatrix}\begin{pmatrix} u \\ v \end{pmatrix} = \begin{pmatrix} 0 \\ 0 \end{pmatrix}.$$

Requiring $(u, v) \neq (0, 0)$, with $\alpha' = \alpha^2 - \beta^2$, we have

$$\epsilon\alpha q^4 + \left(1 + \epsilon\left(\alpha' + \alpha\lambda^2p^2\right)\right)p^2q^2 + \left(\alpha + \lambda^2p^2\right)p^4 = 0.$$

Since we concern the region, $p \ll 1/d$, for a continuum theory, from the relation $\lambda^2 \sim d^2/\epsilon$ we have $\epsilon\lambda^2p^2 \ll 1$ and $\epsilon\lambda p \ll 1$. Then, we arrive at the two solutions,

$$q^2 = -p^2(\alpha + \lambda^2p^2) + O(\epsilon), -\frac{p^2}{\epsilon\alpha}(1 + O(\epsilon)).$$

The minus sign on the right-hand side indicates that the solution is a damping function in the y-direction and some trigonometric function in the x-direction.

From the second solution, we have $v \sim \sqrt{\epsilon}u$. Since we seek the solution with $v > u$ in our boundary condition, we chose the first, *i.e.*, $q^2 = -p^2(\alpha + \lambda^2p^2)$. Thus, at large scale ($\lambda p \ll 1$), we have $q^2 = -p^2\alpha$, which leads to $u \sim \epsilon v$. These facts allow us to reduce equation (7) to the form announced in equation (4). At small scale ($\lambda p \gg 1$), we have $q^2 = -\lambda^2p^4$ and, thus, $u \sim \epsilon\lambda pv$, which allows equation (7) to be reduced to the form in equation (5).

Unlike the perpendicular case [4], the energy is not simplified into a single form over all length scale in the present case. Instead, we observe the simplification of the energy at both the large and small scales, *i.e.* $\lambda p \ll 1$ and $\lambda p \gg 1$. We note here that λ is rather *large* compared with the layer thickness, *i.e.* $\lambda \sim d/\sqrt{\epsilon}$. The ensuing analysis is based on the condition, $d \ll \lambda \ll L$, where $2L$ is the y dimension of the sample.

4 Large scale solution

At equilibrium, by minimizing the energy given in equation (4), we have

$$\left(\frac{\partial^2}{\partial \overline{x}^2}+\frac{\partial^2}{\partial y^2}\right)u_y=0,$$

where

$$\overline{x}=\sqrt{2(1+\nu)}x.$$

When the crack tip is located at the origin of the x-axis the appropriate boundary conditions are, under the fixed condition, as follows:

$$\begin{aligned}u_y&=\pm u_0 \text{ at } y=\pm L,\\ u_y&=0 \text{ for } y=0,\ x\ll 0(x\ll -\lambda),\\ \frac{\partial u_y}{\partial y}&=0 \text{ for } y=0,\ x\gg 0(x\gg \lambda).\end{aligned}$$

Note here that these boundary conditions specify the conditions at the points *away from the origin.* As in the perpendicular case, in analogy with the boundary problem for a variable condenser [4], we have the displacement

$$u_y=\frac{2u_0}{\pi}\operatorname{Im}\left[\log\left(e^{i\pi z/(2L)}+\left(e^{i\pi z/L}-1\right)^{1/2}\right)\right], \quad (8)$$

with

$$z=y+i\left(\overline{x}-\overline{x}_0\right).$$

In the above, the branch of the function $z^{1/2}$ is chosen such that $z^{1/2}=r^{1/2}\exp(i\theta/2)$ with $0<\theta<2\pi$ (*e.g.*, $(-1)^{1/2}=i$). Here, the remote-boundary conditions allow the shift, $x_0\left(=\overline{x}_0/\sqrt{2(1+\nu)}\right)$, in our solution, as far as $x_0\ll L$.

In the following, we consider only the region $y>0$, since the problem is symmetric with respect to the x-axis. When $|z|\ll L$, we have

$$u_y(x,y)=\frac{2u_0}{\pi}\operatorname{Im}\left[\left(\frac{i\pi z}{L}\right)^{1/2}\right]. \quad (9)$$

In the vicinity of the origin (but still $x\gg\lambda$), it reduces to a parabolic form:

$$u_y(x,y=0)=2u_0\theta(x)\sqrt{\frac{\overline{x}-\overline{x}_0}{\pi L}}, \quad (10)$$

where $\theta(x)$ is the Heaviside step function. Here and hereafter, *the notation* $y=0$ *should be understood as the limit where the variable* y *approaches to a positive infinitesimal quantity.* This is because the consideration for the region $y>0$ is enough due to the symmetry.

The nonzero component of the stress field is given from $\sigma_{yy}=E_0e_{yy}$:

$$\sigma_{yy}=\sigma_\infty\operatorname{Re}\left[\frac{e^{i\pi z/(2L)}}{\left(e^{i\pi z/L}-1\right)^{1/2}}\right], \quad (11)$$

where the remote tensile stress is given by

$$\sigma_\infty=E_0\frac{u_0}{L}.$$

When $|z|\ll L$, we have

$$\sigma_{yy}(x,y)=\sigma_\infty\operatorname{Re}\left[\left(\frac{i\pi z}{L}\right)^{-1/2}\right],$$

and stress distribution near the tip is given by

$$\sigma_{yy}(x,y=0)=\sigma_\infty\theta(-x)\sqrt{\frac{L}{\left(-\left(\overline{x}-\overline{x}_0\right)\right)\pi}}. \quad (12)$$

Note here that these expressions are valid only when $x>\lambda(\sim d/\sqrt{\epsilon})$, where $\lambda\ll L$.

5 Small-scale solution

From equation (5), we have a "pseudo *bi-diffusion*" equation,

$$\frac{\partial^2 u_y}{\partial y^2}=\lambda^2\frac{\partial^4 u_y}{\partial x^4}. \quad (13)$$

The solution to our problem has to satisfy the following two boundary conditions at least:

$$\begin{aligned}u_y&=0 \text{ for } y=0,\ x<0(|x|\ll\lambda),\\ \frac{\partial u_y}{\partial y}&=0 \text{ for } y=0,\ x>0(x\ll\lambda).\end{aligned}$$

In addition, the solution should be able to match with the large-scale solution.

5.1 General solution for the boundary problem

The field u_y satisfies the (pseudo) *bi-diffusion* equation

$$\left(\partial_y+\lambda\partial_x^2\right)\left(\partial_y-\lambda\partial_x^2\right)u_y=0.$$

Putting $S_u=\left(\partial_y-\lambda\partial_x^2\right)u_y$, we see that S_u is a solution to the anti-diffusion equation

$$\left(\partial_y+\lambda\partial_x^2\right)S_u=0$$

and that u_y satisfies the inhomogeneous diffusion equation

$$\left(\partial_y-\lambda\partial_x^2\right)u_y=S_u.$$

The source function S_u is a solution of the anti-diffusion equation (a typical solution is $\exp\left(\frac{x^2}{4\lambda y}\right)/\sqrt{4\pi\lambda y}$) and blows up when y approaches to zero, except that S_u is independent of y, *i.e.* $S_u=A+Bx$ (this fact can be confirmed later), where A and B are constants independent of x and y.

Since u_y satisfies the bi-diffusion equation, σ_{yy} also satisfies the bi-diffusion equation. Putting $S_\sigma = \left(\partial_y - \lambda\partial_x^2\right)\sigma_{yy}$, we have

$$\left(\partial_y - \lambda\partial_x^2\right)\sigma_{yy} = S_\sigma.$$

To have a physical solution, we have $S_u = A + Bx$ and we conclude that $S_\sigma = 0$ because $S_\sigma = E_0\partial_y S_u$. Namely, σ_{yy} *is the solution of the diffusion equation.* As we shall see later, the function S_u obtained starting from the diffusion equation for σ_{yy} is actually in the form, $S_u = A + Bx$. In this way, we shall obtain the general solution for u_y.

The general solution for the initial boundary condition (here, "initial" corresponds to $y = 0$)

$$\sigma_{yy}(x, y = 0) = F(x) \tag{14}$$

is given as

$$\sigma_{yy}(x,y) = \frac{1}{\sqrt{4\pi\lambda y}}\int_{-\infty}^{\infty} F(x')\exp\left(-\frac{(x-x')^2}{4\lambda y}\right)\mathrm{d}x'. \tag{15}$$

In the following, we determine *the source function* $F(x)$ considering appropriate boundary conditions. Requiring the boundary condition

$$\sigma_{yy}(x,y) = 0 \qquad \text{for } y = 0 \quad \text{and } x > 0, \tag{16}$$

we may put

$$F(x) = \theta(-x)f(x) + \sigma\lambda\delta(x), \tag{17}$$

where $\delta(x)$ is Dirac's delta-function and $f(x)$ and σ are the quantities to be determined. As we see later, the second singular term in the source function is required to have a smooth matching to the outer solution. In this way, we have

$$\sigma_{yy}(x,y) = \frac{1}{\sqrt{4\pi\lambda y}}\int_{-\infty}^{0} f(x')\exp\left(-\frac{(x-x')^2}{4\lambda y}\right)\mathrm{d}x' + \sigma\sqrt{\frac{\lambda}{4\pi y}}\exp\left(-\frac{x^2}{4\lambda y}\right). \tag{18}$$

By integrating equation (18) over y, we have ($\mathrm{erfc}\,(x) = 1 - \mathrm{erf}(x)$, $\mathrm{erf}(x) = \frac{2}{\sqrt{\pi}}\int_0^x e^{-t^2}\mathrm{d}t$)

$$E_0u_y(x,y) = \int_{-\infty}^{0} f(x') \times\left(\sqrt{\frac{y}{\pi\lambda}}e^{-\frac{(x-x')^2}{4\lambda y}} - \frac{x-x'}{2\lambda}\,\mathrm{erfc}\left(\frac{x-x'}{\sqrt{4\lambda y}}\right)\right)\mathrm{d}x' + \sigma\left(\sqrt{\frac{\lambda y}{\pi}}\exp\left(-\frac{x^2}{4\lambda y}\right) - \frac{x}{2}\,\mathrm{erfc}\left(\frac{x}{\sqrt{4\lambda y}}\right)\right) + C(x), \tag{19}$$

where we have used the formula given in [17,18], in which formulae the integration constants are chosen so that the result vanishes at $x = -\infty$. In the above, $C(x)$ is the solution of the bi-diffusion equation independent of y, *i.e.*

$$C(x) = c_0 + c_1x + c_2x^2 + c_3x^3.$$

The boundary condition required for $u_y(x,y)$ is

$$u_y(x,y) = 0 \text{ for } y = 0 \text{ and } x < 0. \tag{20}$$

To determine the function $f(x)$ to accommodate this boundary condition, we consider $u_y(x,y)$ at $y = 0$. Noting the relation

$$\int_{-\infty}^{0} f(x')\frac{x-x'}{2\lambda}\,\mathrm{erfc}\left(\frac{x-x'}{2\sqrt{\lambda y}}\right)\mathrm{d}x' = \left(\int_{-\infty}^{x}\mathrm{d}x' + \int_{x}^{0}\mathrm{d}x'\right) f(x')\frac{x-x'}{2\lambda}\,\mathrm{erfc}\left(\frac{x-x'}{2\sqrt{\lambda y}}\right),$$

where the first term in the right-hand side is zero at $y = 0$ and the second term is nonzero only when $x < 0$, we have

$$E_0u_y(x, y = 0) = \theta(-x)\left(\frac{1}{\lambda}\int_0^x f(x')(x-x')\,\mathrm{d}x' - \sigma x\right) + C(x).$$

Here, note the relation $\mathrm{erfc}\left((x-x')/\sqrt{4\lambda y}\right) \longrightarrow 2\theta(-x)$ when $y \to 0^+$.

Since $\theta(-x) = 1 - \theta(x)$, the boundary condition (20) is satisfied only when

$$C(x) = \sigma x - \frac{1}{\lambda}\int_0^x f(x')(x-x')\,\mathrm{d}x', \tag{21}$$

to have

$$E_0u_y(x, y = 0) = \theta(x)\left(\sigma x - \frac{1}{\lambda}\int_0^x f(x')(x-x')\,\mathrm{d}x'\right).$$

Condition (21) is strong in the sense that $C(x)$ is the polynomial of x with the order lower than the fourth and is independent of y; $f(x)$ should be at most linear in x,

$$f(x) = a_0 + a_1x. \tag{22}$$

In this way, we obtain

$$E_0u_y(x, y = 0) = \theta(x)\left(\sigma x - \frac{1}{\lambda}\left(\frac{1}{2}a_0x^2 + \frac{1}{6}a_1x^3\right)\right) \tag{23}$$

and from equations (14) and (17), we have (for $x \neq 0$)

$$\sigma_{yy}(x, y = 0) = \theta(-x)(a_0 + a_1x). \tag{24}$$

6 Matching between inner and outer solutions

Equation (23) contains the three unknown constants, a_0, a_1, and σ, while the outer solution one unknown x_0; there are four unknowns. To determine these constants we require that u_y and $\partial_x u_y$ match the outer solution at $x = \lambda$, while σ_{yy} and $\partial_x\sigma_{yy}$ match the large-scale solution at $x = -\lambda$.

6.1 Outer solution

Introducing α (which is different from α used in Sect. 3),

$$\alpha^2 = \sqrt{2\,(1+\nu)},$$

we have

$$\begin{aligned} u_y(x,y=0) &= 2u_0\alpha\theta(x)\sqrt{\frac{x-x_0}{\pi L}}, \\ \frac{\partial}{\partial x}u_y(x,y=0) &= \theta(x)\frac{u_0\alpha}{\sqrt{\pi L\,(x-x_0)}}, \\ \frac{1}{E_0}\sigma_{yy}(x,y=0) &= \theta(-x)\frac{u_0}{\alpha\sqrt{\pi L\,(-(x-x_0))}}, \\ \frac{1}{E_0}\frac{\partial}{\partial x}\sigma_{yy}(x,y=0) &= \theta(-x)\frac{u_0}{2\alpha\sqrt{\pi L}}\left(-(x-x_0)\right)^{-3/2}. \end{aligned}$$

6.2 Inner solution

Introducing a, b and u (which is different from u in Sect. 3),

$$a \equiv \frac{\lambda a_0}{E_0 u}, \quad b \equiv \frac{a_1\lambda^2}{E_0 u}, \quad u \equiv \frac{\sigma\lambda}{E_0},$$

we have

$$\begin{aligned} u_y(x,y=0) &= u\theta(x)\left(\frac{x}{\lambda} - \left(\frac{a}{2\lambda^2}x^2 + \frac{b}{6\lambda^3}x^3\right)\right), \\ \frac{\partial}{\partial x}u_y(x,y=0) &= u\theta(x)\left(\frac{1}{\lambda} - \left(\frac{a}{\lambda^2}x + \frac{b}{2\lambda^3}x^2\right)\right), \\ \frac{1}{E_0}\sigma_{yy}(x,y=0) &= \theta(-x)\frac{u}{\lambda}\left(a + \frac{b}{\lambda}x\right), \\ \frac{1}{E_0}\frac{\partial}{\partial x}\sigma_{yy}(x,y=0) &= \theta(-x)u\frac{b}{\lambda^2}. \end{aligned}$$

6.3 Matching

We have four conditions, while we have four unknowns, a, b, x_0, and u, for the four conditions.

At $x=\lambda$:

$$\begin{aligned} -u\left(\frac{a}{2} + \frac{b}{6}\right) + u &= 2\alpha u_0 l\sqrt{\gamma}, \\ -u\left(\frac{a}{\lambda} + \frac{b}{2\lambda}\right) + u\frac{1}{\lambda} &= \frac{\alpha u_0 l}{\lambda\sqrt{\gamma}}. \end{aligned}$$

Here, we have introduced

$$l = \sqrt{\frac{\lambda}{\pi L}}, \gamma = 1 - \frac{x_0}{\lambda}.$$

At $x=-\lambda$:

$$\begin{aligned} \frac{u}{\lambda}(a-b) &= \frac{u_0 l}{\alpha\lambda\sqrt{\gamma'}}, \\ u\frac{b}{\lambda^2} &= \frac{u_0 l}{2\alpha\lambda\lambda^2\left(\sqrt{\gamma'}\right)^3}. \end{aligned}$$

Here, we have introduced

$$\gamma' \equiv 1 + \frac{x_0}{\lambda}$$

from which we have $-x + x_0 = \lambda(1 + x_0/\lambda) = \lambda\gamma'$. With the definition

$$\eta = \frac{u_0}{u}l,$$

we have

$$\begin{cases} a = 4 - 2\alpha\eta\dfrac{6\gamma - 1}{\sqrt{\gamma}}, \\ b = -6 + 6\alpha\eta\dfrac{4\gamma - 1}{\sqrt{\gamma}} \end{cases} \tag{25}$$

and

$$\begin{cases} a = \eta\dfrac{2\gamma' + 1}{2\alpha(\gamma')^{\frac{3}{2}}}, \\ b = \dfrac{\eta}{2\alpha(\gamma')^{\frac{3}{2}}}. \end{cases}$$

Thus, we have a set of equations for γ and η:

$$\begin{cases} 4 - 2\alpha\eta\dfrac{6\gamma - 1}{\sqrt{\gamma}} = \eta\dfrac{2\gamma' + 1}{2\alpha(\gamma')^{\frac{3}{2}}}, \\ -6 + 6\alpha\eta\dfrac{4\gamma - 1}{\sqrt{\gamma}} = \dfrac{\eta}{2\alpha(\gamma')^{\frac{3}{2}}}. \end{cases} \tag{26}$$

The numerical solution to this set of equations with $|x_0| < \lambda$ (or $|1-\gamma| < 1$) is $\gamma = 0.72, \eta = 0.39$ for $\nu = 0$ and $\eta = 0.38, \gamma = 0.67$ for $\nu = 1/2$.

Approximate but analytical expressions for them can be obtained as follows. Introducing $\eta' \equiv 1/\eta$ and δ by

$$\delta = x_0/\lambda, \gamma = 1 - \delta, \gamma' = 1 + \delta$$

and, assuming, $\delta \ll 1$, the set of equations can be reduced to

$$\begin{cases} 4\eta' - 2\alpha\left(5 - \dfrac{7}{2}\delta\right) = \dfrac{6 - 5\delta}{4\alpha}, \\ -6\eta' + 6\alpha\left(3 - \dfrac{5}{2}\delta\right) = \dfrac{2 - 3\delta}{4\alpha}. \end{cases}$$

Solving this set of equations we have an approximate solution:

$$\begin{cases} \delta = \dfrac{2\left(12\alpha^2 - 11\right)}{3\left(12\alpha^2 - 7\right)}, \\ \eta' = \dfrac{48\alpha^4 - 8\alpha^2 - 1}{3\left(12\alpha^2 - 7\right)\alpha}. \end{cases}$$

For $\alpha = \sqrt{2(1+\nu)}$ with $0 < \nu < 1/2$, $\delta \simeq 0.4$ which barely justifies the assumption $\delta \ll 1$, while $\eta' \simeq 2.4$. In this way, we confirm that γ *and* η *are both positive quantities of the order of unity* for any value of ν ($0 < \nu < 1/2$).

7 Overall solution

For $|x| < \lambda$, from equations (19, 21) and (22) we have

$$\frac{u_y(x,y)}{u} = -\frac{1}{2}\left(\frac{a}{2}X^2 + \frac{b}{6}X^3\right)\left(1 + \mathrm{erf}\left(\frac{X}{\sqrt{4Y}}\right)\right) + \frac{1}{2}Y\,(a + bX)\,\mathrm{erfc}\left(\frac{X}{\sqrt{4Y}}\right) - \left(\frac{2}{3}bY + \frac{\frac{a}{2}X^2 + \frac{b}{6}X^3}{X}\right)\sqrt{\frac{Y}{\pi}}e^{-\frac{X^2}{4Y}} \qquad (27)$$

and from equations (18) and (22) we have

$$\frac{\sigma_{yy}(x,y)\lambda}{E_0} = \frac{1}{2}\,(a + bX)\,\mathrm{erfc}\left(\frac{X}{\sqrt{4Y}}\right) - b\sqrt{\frac{Y}{\pi}}e^{-\frac{X^2}{4Y}},$$

where a (~ 0.4) and b (~ 0.1) are given by equations (25) and $u = u_0 l/\eta$ ($\sim 2.6u_0 l$) with γ and η given by equations (26). Here, $X = x/\lambda$ and $Y = y/\lambda$.

For $|x| > \lambda$, u_y and σ_{yy} are given by equations (8) and (11), where $x_0 = (1-\gamma)\lambda$ ($\sim 0.3\lambda$).

As expected and clear from (27), these expressions are only valid for $y \ll \lambda$ (at small scale, we have $q^2 = -\lambda^2 p^4$ with $\lambda p \gg 1$, from which we have $q^2 \gg p^2 \gg 1/\lambda$).

If we operate $\left(\partial_y - \lambda\partial_x^2\right)$ to the right-hand side of equation (27), we obtain $a + bX$, which corresponds to S_u in the previous section and thus confirms the statement mentioned there.

A typical shape of the crack tip and stress distribution around the surface ($0 < y \ll \lambda$) is given in the plots in Figure 2 with the parameters given in Section 8. The solution becomes precise only when $x \ll \lambda$ or $x \gg \lambda$. Near the tip ($x \ll \lambda$), the tip is *lenticular* ($\sim x$) while away from the tip ($x \gg \lambda$), the deformation field recovers the ordinary square-root law ($\sim \sqrt{x}$) [19–21].

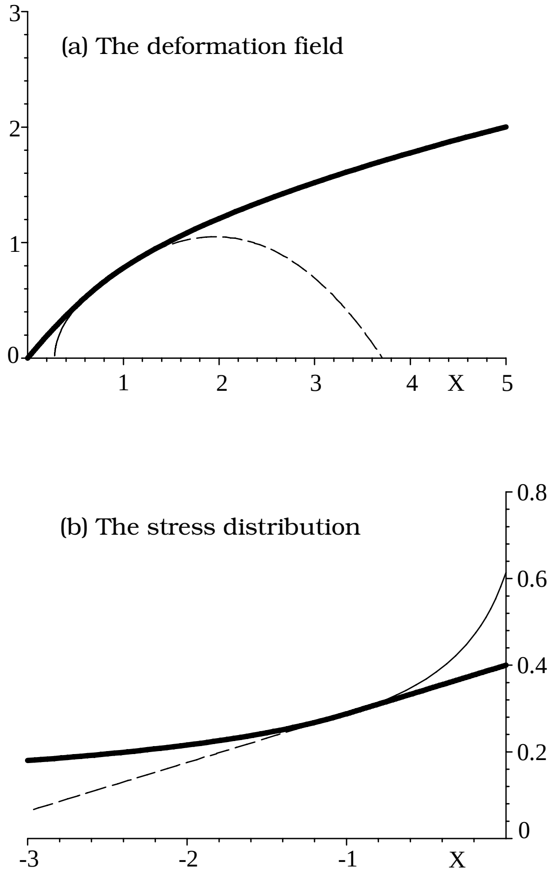

Fig. 2. Crack shape (a) and stress distribution (b) for a parallel crack. The bold line corresponds to the overall solution, while the fine line and the broken line correspond to the large-scale solution and the small-scale solution, respectively. The overall solution becomes exact only when $x \ll \lambda$ or $x \gg \lambda$. Near the tip ($x \ll \lambda$), the tip is a linear function ($\sim x$), while, away from the tip ($x \gg \lambda$), the deformation field recovers the ordinary square-root law ($\sim x^{1/2}$). The parameters used for the numerical calculation are $d = 1\,\mu$m, $L = 1$ cm, and $\lambda = 250\,\mu$m, where $\epsilon = 1/250$, $L/\lambda = 40$, and $d/\lambda = 1/250$ (see Sect. 8).

8 Discussion

Since we have the usual singular behavior for the stress and stress fields we have

$$G_0 \sim (\sigma u)_{\text{large scale}} \sim \sigma_\infty u_0. \qquad (28)$$

On the other hand, from Griffith's energy balance, we have $\gamma_0 \sim L\sigma_\infty^2/E_0$ [5]. Thus, the fracture energy is of the order of γ_0 as predicted by the scaling consideration.

Since we have

$$\overline{\theta}_0(x) \equiv \frac{\partial}{\partial x}u_y(x, y=0) = u\theta(x)\left(\frac{1}{\lambda} - \left(\frac{a}{\lambda^2}x + \frac{b}{2\lambda^3}x^2\right)\right),$$

the crack tip angle at $x = 0$ is

$$\theta_0 \equiv \overline{\theta}_0(0) = \frac{u_0 l}{\eta\lambda} \sim \frac{u_0}{\sqrt{L\lambda}}.$$

By rewriting the last expression with the aid of equation (28), we have

$$\theta_0 \sim \sqrt{\frac{\gamma_0}{E_0\lambda}}$$

as predicted in equation (6).

Typical parameters for nacre are as follows:

$$d = 1\ \mu\text{m}\,,\quad L = 1\ \text{cm}\,,\quad \epsilon = 1/250\,.$$

For these parameters we have

$$\lambda = 250\ \mu\text{m}\,,\quad L/\lambda = 40\,,\quad d/\lambda = 1/250\,.$$

These numerical values allow us the continuum description with length scales λ and L since the relation $d \ll \lambda \ll L$ holds for these values.

If we did not include the last term in equation (17), we would not have a linear term in the deformation field and this would contradict the scaling expectation (in addition, we could not make a smooth matching as we see below); we would have

$$\begin{cases} u_y = -u\left(\dfrac{a}{2\lambda^2}x^2 + \dfrac{b}{6\lambda^3}x^3\right)\theta(x)\,, \\ \dfrac{1}{E_0}\sigma_{yy} = \dfrac{u}{\lambda}\left(a + \dfrac{b}{\lambda}x\right)\theta(-x)\,. \end{cases} \tag{29}$$

Here, we have only two unknowns; $a' \equiv ua$ and $b' \equiv ub$. Let us assume first that $a' \neq 0$. Then, the first equation implies $a' < 0$ for a positive u_y around the origin ($x = 0$), while the second equation implies $a' > 0$ for a positive σ_{yy}. (We have assumed $u > 0$.) Thus, for consistency, we have $a' = 0$.

Thus, we have

$$\begin{cases} u_y(x,y) = -\dfrac{b'}{6\lambda^3}x^3\theta(x)\,, \\ \dfrac{1}{E_0}\sigma_{yy} = \dfrac{b'}{\lambda^2}x\theta(-x)\,. \end{cases}$$

For positive u_y and σ_{yy}, we have $b' < 0$. By introducing the shift x_0 for the outer solution as before, the matching of both the fields themselves is possible. However, since the inner solution u_y ($\sim x^3$) is concave (positive curvature) while the outer solution ($\sim \sqrt{x}$) convex (negative curvature), the smooth matching is impossible. For a similar reason, the smooth matching of the stress is also impossible and the stress field at $x = 0$ tends to zero. These facts suggest the need for the last term in equation (17).

9 Conclusion

In this paper, we have developed a continuum theory for a nanoscale layered structure with a parallel crack. We indicated the importance of the bending term near the crack, which leads to a parabolic differential equation and, thereby, a lenticular tip form. From the coarse-grained view, we have a simplified picture with analytical expressions; the deformation field is a linear function of x (the distance from the tip) near the tip and goes back to the usual square-root function of x away from the tip. As a result, the fracture energy of nacre against the parallel crack is of the same order as the soft organic material; there is no enhancement in toughness within our simplified view.

The author is grateful to Pierre-Gilles de Gennes for a number of essential discussions at the early stage of this work. He would like to express his sincere gratitude to all the members of de Gennes' group at Collège de France for warm hospitality during his stay in Paris. He also thanks Elie Raphaël for discussions. This work is supported by Joint Research Project between Japan Society for the Promotion of Science (JSPS) and Centre National de la Recherche Scientifique (CNRS).

References

1. T. Kelly, B. Clyne, Phys. Today **52**, 37 (1999).
2. W.J. Clegg, Science **286**, 1097 (1999).
3. R. Naslain, B. Harris (Editors), *Ceramic Matrix Composites: Components, Preparation, Microstructure and Properties* (Elsevier Applied Science, 1989); A.G. Evans, R. Naslain (Editors), *High-Temperature Ceramic-Matrix Composites (I, II)* (American Ceramic Society, 1994, 1995); S.T. Mileiko, *Metal and Ceramic Based Composites* (Elsevier Science Ltd., 1997); K.K. Chawla, K.K. Chawla, *Composite Materials: Science and Engineering* (Springer-Verlag, 1998); A. Kelly, N.H. Macmillan, *Strong Solids* (Oxford University Press, Oxford, 1986); D. Hull, T.W. Clyne, *An Introduction to Composite Materials* (Cambridge University Press, Cambridge, 1993).
4. K. Okumura, P.-G. de Gennes, Eur. Phys. J. E **4**, 121 (2001).
5. P.-G. de Gennes, K. Okumura, C. R. Acad. Sci. Paris t. **1**, Ser. IV, 257 (2000).
6. J.D. Currey, Proc. R. Soc. London Ser. B **196**, 443 (1977).
7. A.P. Jackson, J.F.V. Vincent, R.M. Turner, Proc. R. Soc. London Ser. B **234**, 415 (1988).
8. M. Sarikaya, J. Liu, I.A. Aksay, *Biomimetics: Design and Processing of Materials*, (AIP Press, New York, 1995) pp. 35-90.
9. M.P. Rao, A.J. Sánchez-Herencia, G.E. Beltz, R.M. McMeeking, F.F. Lange, Science **286**, 102 (1999).
10. D. Leguillon, E. Sanchez-Palencia, *Fracture in Heterogeneous Materials*, in *New Advances in Computational Structural Mechanics*, edited by P. Ladevèze, O.C. Zienkiewicz (Elsevier, 1992) p. 423; Int. J. Fract. **99**, 25 (1999).
11. P.G. de Gennes, *The Physics of Liquid Crystal* (Clarendon Press, Oxford, London, 1974).
12. P.G. de Gennes, Europhys. Lett. **13**, 709 (1990).
13. L.D. Landau, E.M. Lifshitz, *Theory of Elasticity*, 3rd edition (Butterworth-Heinemann, 1995).
14. A.A. Griffith, Phil. Trans. R. Soc. London A **221**, 163 (1920).
15. P.G. de Gennes, *Scaling Concepts in Polymer Physics* (Cornell University Press, Ithaca, 1979).
16. P.G. de Gennes, F. Brochard-Wyart, D. Quéré, *Gouttes, bulles, perles et ondes* (Belin, Paris, 2002).
17. $\int\left(\frac{1}{\sqrt{4\pi\lambda y}}\exp\left(-\frac{(x-x')^2}{4\lambda y}\right)\right)\mathrm{d}y = \sqrt{\frac{y}{\pi\lambda}}e^{-\frac{(x-x')^2}{4\lambda y}} - \frac{x-x'}{2\lambda}\,\mathrm{erfc}\left(\frac{x-x'}{\sqrt{4\lambda y}}\right)$.
18. $\int\left(\sqrt{\frac{\lambda}{4\pi y}}\exp\left(-\frac{x^2}{4\lambda y}\right)\right)\mathrm{d}y = \sqrt{\frac{\lambda y}{\pi}}\exp\left(-\frac{x^2}{4\lambda y}\right) - \frac{x}{2}\,\mathrm{erfc}\left(\frac{x}{\sqrt{4\lambda y}}\right)$.
19. J.R. Rice, *Fracture: an Advanced Treatise*, edited by H. Liebowitz, Vol. **II** (Academic Press, New York, 1968) pp. 191-311.
20. T.L. Anderson, *Fracture Mechanics-Fundamentals and Applications* (CRC Press, Boca Raton, 1991).
21. B. Lawn, *Fracture of Brittle Solids*, 2nd edition (Cambridge University Press, New York, 1993).